Journal of Physics: Conference Series **500** (2014) 152016 doi:10.1088/1742-6596/500/15/152016

Combined Hydrodynamic and Diffraction Simulations of Femtosecond X-ray Scattering from Laser-Shocked Crystals

Justin S. Wark[1], **Andrew Higginbotham**[1], **Despina Milathianaki**[2] **and Arianna Gleason**[3]

[1] Department of Physics, Clarendon Laboratory, Parks Road, University of Oxford, Oxford, OX1 3PU, United Kingdom
[2] Linac Coherent Light Source (LCLS), SLAC National Accelerator Laboratory, 2575 Sand Hill Road, Menlo Park, CA 94025, USA
[3] Department of Geological & Environmental Sciences, Stanford University, Stanford, CA 94305 USA

E-mail: justin.wark@physics.ox.ac.uk

Abstract. We describe a simple hydrocode based on a two-step integration scheme that models the evolution of elastic and plastic strains in crystals subject to rapid laser-shock loading. By monitoring the elastic strains during plastic flow we track the rotation and spacing of lattice planes within the polycrystalline sample, and can thus predict the signal that would be produced by x-ray diffraction in a variety of experimental geometries. By employing a simple Taylor-Orowan dislocation model we simulate diffraction patterns in a Debye-Scherrer geometry to track the orthogonal strain states within a laser-shocked sample. The yielding rate is approximately matched to those observed in multi-million atom molecular dynamics (MD) simulations, allowing movies to be made of the diffraction images that would be seen in a real experimental geometry, and illustrating the pertinent experimental requirements, including target texture. Judicious choice of geometry allows clear demarcation of the initial elastic response of the target to be made from the subsequent plastic relaxation. We discuss the simulations in the context of the novel experimental capabilities that have recently become available with the advent of 4^{th} generation light sources, which allow single-shot diffraction with sub-100-fsec resolution.

1. Introduction

The use of short-pulses of x-rays to interrogate laser-shocked crystals has a long history, with laser-plasma based x-ray sources first being used both to interrogate the response of single crystals on nanosecond time-scales [1, 2, 3], and then further developed to allow diffraction in powder geometry, so that polycrystalline samples could be studied [4, 5]. The majority of these studies used x-ray sources several hundreds of picoseconds, to several nanoseconds in duration. However, the advent of 4^{th} generation light sources such as the Linac Coherent Light Source (LCLS) [6, 7] provides the opportunity to study shocked materials via *in situ* x-ray diffraction with unprecedented temporal resolution, as single shot powder diffraction images can be now obtained with exposures far below 100-fsec, even shorter than the period of the most energetic phonon in the system.


Content from this work may be used under the terms of the Creative Commons Attribution 3.0 licence. Any further distribution of this work must maintain attribution to the author(s) and the title of the work, journal citation and DOI.
Published under licence by IOP Publishing Ltd

We thus now have the capability to perform experiments on the same length and time-scales as those that pertain to multi-million atom molecular dynamics (MD) simulations [8], and the post-processing of MD simulations to provide diffraction has been shown to be a productive method of determining the physical mechanisms that are active at the lattice level during shock compression [9]. Whilst MD provides the most detailed insight into the physics at the lattice level, hydrodynamic simulations at the continuum level have the advantage of being extremely rapid to perform, and thus can quickly provide insight into how lattice deformation will manifest itself in diffraction images. In this context we present here a simple two-step hydrodynamic model of the elastic strains present in a micron-scale sample shocked to several tens of GPa on picosecond time-scales - i.e. precisely the type of conditions that are well-suited to 4^{th} generation light source studies. Given a plasticity model, the hydrocode predicts the evolution of the elastic strains within the sample, both along and perpendicular to the shock propagation direction, and these elastic strains are then used to predict the instantaneous diffraction patterns in a Debye-Scherrer geometry.

2. Simulation Method

2.1. The Hydrodynamic Equations

Conservation of mass and momentum lead to the well-known equations relating stress along the (normal) shock direction, σ_{n}, the total strain, elastic plus plastic, along the normal direction, $\epsilon_{\text{n}} = \epsilon_{\text{n}}^{\text{e}} + \epsilon_{\text{n}}^{\text{p}}$, and the particle velocity, u:

$$\rho_0 \left(\frac{\partial u}{\partial t}\right) + \left(\frac{\partial \sigma_{\text{n}}}{\partial z}\right) = 0 \quad , \tag{1}$$

$$\left(\frac{\partial \epsilon_{\text{n}}}{\partial t}\right) + \left(\frac{\partial u}{\partial z}\right) = 0 \quad , \tag{2}$$

where ρ_0 is the ambient density of the material. Plastic flow is incorporated into a relaxation function, $g(\sigma_{\text{n}}, \epsilon_{\text{n}})$, such that

$$\left(\frac{\partial \sigma_{\text{n}}}{\partial t}\right) - \left(K + \frac{4\mu'}{3}\right)\left(\frac{\partial \epsilon_{\text{n}}}{\partial t}\right) = -g(\sigma_{\text{n}}, \epsilon_{\text{n}}) \quad , \tag{3}$$

where K is the bulk modulus of the material (which we assume is non linear, and a function of pressure, i.e. $K = K_0 + K_1 P$), and μ' is an effective shear modulus. That is to say, if the material were completely isotropic, one could use the standard shear modulus, but if the target is highly textured, such that the crystallites within the sample were strongly preferentially oriented along a particular direction, then this should be taken into account in determining the value of μ'.

A finite value of g gives rise to plastic flow, yet we know that the stresses normal and transverse to the shock propagation direction are supported by the elastic components of strain, that is to say

$$\sigma_{\text{n}} = \left(K + \frac{4\mu'}{3}\right)\epsilon_{\text{n}}^{e} + \left(2K - \frac{4\mu'}{3}\right)\epsilon_{\text{t}}^{e} \quad , \quad \sigma_{\text{t}} = \left(K - \frac{4\mu'}{3}\right)\epsilon_{\text{n}}^{e} + \left(2K + \frac{4\mu'}{3}\right)\epsilon_{\text{t}}^{e} \quad . \tag{4}$$

By imposing a time-dependent stress, $\sigma_{\text{n}}(z = 0, t)$ onto a sample, equations 1 to 4 can be solved to provide the stresses, and the normal and transverse components of the elastic and plastic strains as a function of depth within the sample, for a given relaxation function.

2.2. The Relaxation Function

For illustrative purposes we outline here perhaps the simplest form of relaxation function due to Taylor and Orowan [10], which essentially assumes that beyond some threshold stress, dislocation

multiplication occurs, and plastic flow is mediated by these dislocations that have a velocity that is a function of the shear stress. We denote the plastic strain by $\gamma = (\epsilon_{\rm n}^{\rm p} - \epsilon_{\rm t}^{\rm p})/2$, and shear stress $\tau = (\sigma_{\rm n} - \sigma_{\rm t})/2$. The plastic strain rate is determined by Orowan's equation, $\dot{\gamma} = Nbv$, where N is the number of mobile dislocations, b the magnitude of the burger's vector, and v the dislocation velocity. We assume N multiplies due to the shear strain from an intial value N_0, such that $N = N_0 + \alpha\gamma$. Furthermore, the velocity of the dislocations depends on the shear stress, asymptoting to the limit v_∞ according to $v = v_\infty \exp[-(\tau_0 + \phi\gamma)/\tau]$, where ϕ takes into account work hardening. Taken together, and as shown by Horie [11], the above model results in a relaxation function given by

$$g(\sigma_{\rm n}, \epsilon_{\rm n}) = \left(\frac{8\mu b v_\infty}{3}\right)\left\{N_0 + \frac{3\alpha}{8\mu'}\left[\left(K + \frac{4\mu'}{3}\right)\epsilon_{\rm n} - \sigma_{\rm n}\right]\right\} f(\sigma, \epsilon) \tag{5}$$

where

$$f(\sigma, \epsilon) = \exp\left\{-\frac{\tau_0 + \left(\frac{3\phi}{8\mu'}\right)\left[\left(K + \frac{4\mu'}{3}\right)\epsilon_{\rm n} - \sigma_{\rm n}\right]}{3[\sigma_{\rm n} - K\epsilon_{\rm n}]/4}\right\} \tag{6}$$

Furthermore, we assume that $g(\sigma_{\rm n}, \epsilon_{\rm n}) = 0$ below some threshold stress, which determines the elastic limit of the material.

2.3. Integration Scheme

A simple two-step method for solving the above equations has been given by Horie and co-workers [11, 12]. As it is fully described by them, for brevity we simply quote here the final result. In this method two parallel sets of meshes are used, staggered by $\Delta z/2$, $\Delta t/2$. The total normal strain at the lagrangian element with spatial index j, and for time-step $(n+1)$ is related to the normal stress by

$$\epsilon_j^{n+1} = \epsilon_j^n + (R^2/\rho_0)\sum_{m=0}^{n}(\sigma_{j+1}^m - 2\sigma_j^m + \sigma_{j-1}^m) \tag{7}$$

and the stresses are updated by

$$\sigma_j^{n+1} = \sigma_j^n + \left\langle C_L^2 \right\rangle R^2 \sum_{m=0}^{n}(\sigma_{j+1}^m - 2\sigma_j^m + \sigma_{j-1}^m) - \langle g(\sigma, \epsilon)\rangle \Delta t \quad , \tag{8}$$

where $R = \Delta t/\Delta z$, $\rho_0 C_L^2 = (K + 4\mu'/3)$, and $\langle Z\rangle = (Z^{n+1} + Z^n)/2$. Given the total stresses and strains along the normal direction, the composite elastic and plastic components can be deduced using equation 4.

2.4. Simulating Diffraction

The hydrodynamic simulation produces values of the elastic and plastic strains, both normal and transverse to the shock propagation direction ($\epsilon_{\rm n}^{\rm e}$, $\epsilon_{\rm t}^{\rm e}$, $\epsilon_{\rm n}^{\rm p}$, $\epsilon_{\rm t}^{\rm p}$), for each lagrangian element. We recall that the strain is uniaxial, so that $\epsilon_{\rm t} = \epsilon_{\rm t}^{\rm e} + \epsilon_{\rm t}^{\rm p} = 0$, and that plastic dilatation is zero: $\epsilon_{\rm n}^{\rm p} + 2\epsilon_{\rm t}^{\rm p} = 0$, which further implies all volume changes are due to elastic strain: $\epsilon_{\rm n}^{\rm e} + 2\epsilon_{\rm t}^{\rm e} = -\Delta V/V_0$ [13]. Importantly, apart from very small shifts due to certain defects such as stacking faults, x-ray diffraction is only sensitive to elastic strain [14]. Indeed, given compression under unaxial total strain, this marks out x-ray diffraction as a unique diagnostic, in that a measure of the elastic strain transverse to the shock propagation direction is effectively also a measurement of the transverse plastic strain, in that they are by definition then equal and opposite.

We assume that the shocked target is polycrystalline, and that the x-rays are incident parallel to the surface normal (the more general solution, where the shock propagation direction and incident x-rays are non-parallel, is dealt with elsewhere [15]). Most polycrystalline samples are highly textured, and the texture is a function of the manufacture and processing methods. Here we assume that the grains within the sample are strongly oriented along a particular direction (the [111] direction), so that a single value of the effective shear modulus, consisent with this direction, is appropriate. However, we further assume that the degree of texture is such that the range of available grain orientations is sufficient that diffraction will occur with equal probability for both the strained and unstrained samples. In practice, texture maps (pole plots) of the samples will be required to assess the diffracted intensity as a function of angle if the sample is very highly oriented.

Consider an arbitrary vector $\mathbf{A}$ connecting any two lattice points in real space within the unperturbed crystal. Under shock deformation of the crystal along the z axis the direction and magnitude of this vector will change to a value $\mathbf{A'}$ such that

$$\mathbf{A'} = \mathbf{FA} = \begin{bmatrix} (1+\epsilon_{\mathrm{t}}^{\mathrm{e}}) & 0 & 0 \\ 0 & (1+\epsilon_{\mathrm{t}}^{\mathrm{e}}) & 0 \\ 0 & 0 & (1+\epsilon_{\mathrm{n}}^{\mathrm{e}}) \end{bmatrix} \mathbf{A} \quad , \tag{9}$$

and hence $\mathbf{A}{=}\mathbf{F^{-1}A'}$. Now, as reciprocal space is the inverse of real space, it follows that a reciprocal lattice vector in the undisturbed crystal, $\mathbf{G_0}$, is changed by the shock compression to a value $\mathbf{FG'} = \mathbf{G_0}$. Consider diffraction from a particular set of lattice planes in the shocked crystal, such that the Bragg condition is matched at an angle θ_{B}. In the chosen geometry the system is azimuthally symmetric, so the reciprocal lattice vector can be written in the form $\mathbf{G'} = [\sin(2\theta_{\mathrm{B}}),\ 0,\ \cos(2\theta_{\mathrm{B}}) - 1]$. Thus, as $\mathbf{G_0} \cdot \mathbf{G_0} = (\mathbf{FG'}) \cdot (\mathbf{FG'})$, and denoting the Bragg angle for the unshocked lattice as θ_0, we find

$$\sin^4\theta_{\mathrm{B}}[(1+\epsilon_{\mathrm{n}}^{\mathrm{e}})^2 - (1+\epsilon_{\mathrm{t}}^{\mathrm{e}})^2] + \sin^2\theta_{\mathrm{B}}[(1+\epsilon_{\mathrm{t}}^{\mathrm{e}})^2] = \sin^2\theta_0 \quad . \tag{10}$$

Hence, given the elastic strains from the hydrocode, by solving this quartic we can deduce the angle at which a particular lagrangian element diffracts the x-rays.

It is instructive to consider the results of equation 10 in the limits of purely hydrostatic, and purely elastic compression. If the crystal yields completely under compression, such that the hydrostatic limit is attained, then $\epsilon_{\mathrm{n}}^{\mathrm{e}} = \epsilon_{\mathrm{t}}^{\mathrm{e}}$, and $\sin\theta_{\mathrm{B}}(1+\epsilon_{\mathrm{n}}^{\mathrm{e}}) = \sin\theta_0$, which for small strains and angular deviations reduces to a simple differentiation of Bragg's law: $\Delta\theta = -\tan\theta_0\ \epsilon_{\mathrm{n}}^{\mathrm{e}}$. In contrast, if the crystal is compressed along the normal direction elastically, such that there is no plastic deformation, then $\epsilon_{\mathrm{t}}^{\mathrm{e}} = 0$, and in the limit of small strains we find $\Delta\theta = -\sin^2\theta_0\ \tan\theta_0\ \epsilon_{\mathrm{n}}^{\mathrm{e}}$. Thus we see that if the original Bragg angle is relatively small, the experimental set-up is far more sensitive to plastic strain, and this can be used to our advantage to separate the intially purely elastic response of the crystal on short time-scales from the subsequent plastic flow, as will be illustrated in the simulations below.

3. Results of Simulations

Multi-million atom MD simulations of shock-compressed copper predict that on very short (picosecond) time-scales the crystal can withstand extremely high shear stresses before yielding, leading to elastic strains between 15 and close to 20% [8, 16]. If we assume that the sample is highly textured, with the peak of the crystallite texture function lying along the [111] direction, then the peak of the diffraction from $[1\bar{1}1]$ will occur if the x-rays are tuned such that $\theta_0 \approx 19.47°$, and the scattering angle is twice this (i.e., for copper, an x-ray photon energy of 8.92 keV, conveniently just below the K-edge at 8.98 keV, such that minimal absorption, and subsequent

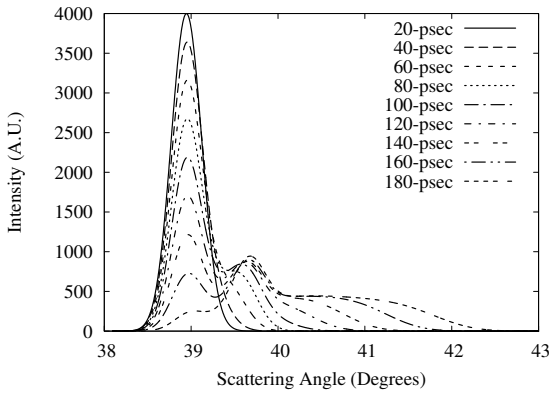

Figure 1. The diffracted x-ray signal as a function of angle as the strain wave, shown in figure 2, progresses into the 1-μm thick copper crystal.

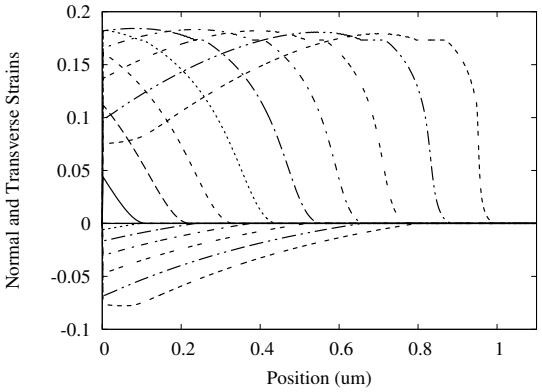

Figure 2. The strains as a function of depth within the crystal, where the positive values correspond to $\epsilon_{\rm n}^{\rm e}$, and the negative values to $\epsilon_{\rm t}^{\rm p}$.

fluorescence, occurs). Note, in an experiment, depending on the degree of texture, one could tune around this x-ray energy and still obtain good data.

In figures 1 and 2 we show the calculated diffracted intensity and strains within the crystal, where we have assumed that it has been irradiated by an approximately Gaussian laser pulse, with FWHM of 80-psec (we have used a separate laser-plasma hydrocode to estimate how the Gaussian intensity of the laser is converted into a time-dependent stress pulse) [17]. In these simulations we use values of the bulk moduli, and the effective (directionally dependent) shear modulus extracted from MD simulations using the Sheng potential [18]. As in the work of Germann [16], we assume completely elastic response of the material up until a threshold strain, after which the values of N_0 and α have been set such that the plastic strain rate is approximately 10^9 s^{-1}. The simulated diffraction profiles take into account not only the strains calculated according to equation 10, but also the small amount of absorption appropriate to each lagrangian element as the x-rays traverse, and are scattered within, the 1-μm thick copper sample. We note that these instantaneous diffraction profiles correspond to those that could be recorded with an x-ray laser source such as LCLS, as the sub 100-fsec duration x-ray pulse is shorter than any phonon period: during such a timescale the compression wave advances less than an interatomic spacing. As the LCLS FEL has a natural bandwidth of order 0.5%, we have convolved the calculated diffraction profiles with a Gaussian of this bandwidth.

There are several features to note within the simulated diffraction data, and how those features relate to the time-dependent strain profiles. Firstly, we see that the peak associated with the unstrained material (found at a scattering angle of 38.94°) decreases in intensity as expected as the compression wave traverses the sample, reducing the thickness of the uncompressed material as it advances. Secondly, over the course of a few tens of picoseconds, a second peak emerges at a scattering angle of close to 39.7°. This peak is associated with the large, purely elastic strain - the scattering angle is relatively small because of the $\sin^2\theta_0$ factor noted above. Lastly, after the threshold strain is reached, and plasticity commences, we find scattering at larger and larger angles (although the elastic strains are lower, the Debye-Scherrer set up is much more sensitive to the plasticity, as noted above, at these relatively low Bragg angles). We therefore see that this geometry should allow for discrimination between purely elastic response, and plastic flow in future experiments.

4. Summary

In summary, we have presented a simple two-step hydrocode that can be used to solve for elastic and plastic strains within a laser-shocked sample for a given relaxation model. As x-ray diffraction is sensitive to the elastic strains, we can deduce the diffraction angles for monochromatic radiation incident onto a polycrystalline sample in the Debye-Scherrer geometry. We note that with a judicious choice of low Bragg angles, this geometry has a very different sensitivity to purely elastic strains, and the elastic strains present during the subsequent plastic flow. The simulations have been proven to be of direct relevance to laser-driven compression experiments using on ultra-short timescales that use x-ray diffraction as a diagnostic, such as those recently performed at LCLS [7].

5. Acknowledgments

JSW is grateful to EPSRC for support under grant number EP/J017256/1. AH acknowledges funding from AWE.

References

[1] Wark J S, Whitlock R R, Hauer A, Swain J E and Solone P J 1987 *Phys. Rev.* B **35** 9391
[2] Wark J S, Whitlock R R, Hauer A, Swain J E and Solone P J 1989 *Phys. Rev.* B **40** 5705
[3] Kalantar D H *et al.* 2005 *Phys. Rev. Lett.* **95** 075502
[4] Hawreliak J, Lorenzana H E, Remington B A, Lukezic S and Wark J S 2007 *Rev. Sci. Instrum.* **78** 083908
[5] Hawreliak J *et al.* 2011 *Phys. Rev.* B **83** 144114
[6] Emma P *et al.* 2010 *Nat. Photonics* **4** 641
[7] Milathianaki D *et al.* 2013 *Science* **342** 220
[8] Bringa E M *et al.* 2006 *Nat. Materials.* **5** 805
[9] Kimminau G *et al.* 2008 *J. Phys.: Condens. Matter* **20** 505203
[10] Taylor J W 1965 *J. Appl. Phys.* **36** 3146
[11] Horie Y 1969 *J. Appl. Phys.* **40** 5368
[12] Chang H L and Horie Y 1972 *J. Appl. Phys.* **43** 3362
[13] Moreland L W 1959 *Phil. Trans.* **251** 341
[14] Rosolankova K, Wark J S, Bringa E M and Hawreliak J 2006 *J. Phys.: Condens. Matter* **18** 6749
[15] Higginbotham A and McGonegle D 2013 General prediction of debye scherrer diffraction patterns in highly strained samples (*Preprint* `arXiv:1308.4958 [cond-mat.mtrl-sci]`)
[16] Dupont V and Germann T C 2012 *Phys. Rev.* B **86** 134111
[17] Larsen J T and Lane S M 1994 *JQSRT* **51** 179
[18] Sheng H, Kramer M, Cadien A, Fujita T and Chen M 2011 *Phys. Rev.* B **83** 134118